GeroScience (2022) 44:1727–1741
https://doi.org/10.1007/s11357-022-00565-9

ORIGINAL ARTICLE

Cannabinoid receptor 2 activation alleviates diabetes-induced cardiac dysfunction, inflammation, oxidative stress, and fibrosis

Mohanraj Rajesh · Partha Mukhopadhyay · Sándor Bátkai · Muhammad Arif · Zoltán V. Varga · Csaba Mátyás · Janos Paloczi · Andrea Lehocki · György Haskó · Pal Pacher

Received: 23 February 2022 / Accepted: 4 April 2022 / Published online: 22 April 2022

Abstract Diabetes mellitus promotes accelerated cardiovascular aging and inflammation, which in turn facilitate the development of cardiomyopathy/heart failure. High glucose-induced oxidative/nitrative stress, activation of various pro-inflammatory, and cell death pathways are critical in the initiation and progression of the changes culminating in diabetic cardiomyopathy. Cannabinoid 2 receptor (CB_2R) activation in inflammatory cells and activated endothelium attenuates the pathological changes associated with atherosclerosis, myocardial infarction, stroke, and hepatic cardiomyopathy. In this study, we explored the role of CB_2R signaling in myocardial dysfunction, oxidative/nitrative stress, inflammation, cell death, remodeling, and fibrosis associated with diabetic cardiomyopathy in type 1 diabetic mice. Control human heart left ventricles and atrial appendages, similarly to mouse hearts, had negligible CB_2R expression determine by RNA sequencing or real-time RT-PCR. Diabetic cardiomyopathy was characterized by impaired diastolic and systolic cardiac function, enhanced myocardial CB_2R expression, oxidative/nitrative stress, and pro-inflammatory response (tumor necrosis factor-α, interleukin-1β, intracellular adhesion molecule 1, macrophage inflammatory protein-1, monocyte chemoattractant protein-1), macrophage infiltration, fibrosis, and cell death. Pharmacological activation of CB_2R with a selective agonist attenuated diabetes-induced inflammation, oxidative/nitrative stress, fibrosis and cell demise, and consequent cardiac dysfunction without affecting hyperglycemia. In contrast, genetic deletion of CB_2R aggravated myocardial pathology. Thus, selective activation of CB_2R ameliorates diabetes-induced myocardial tissue injury and preserves the functional contractile capacity of the myocardium in the diabetic milieu. This is particularly encouraging, since unlike CB_1R agonists, CB_2R agonists do not elicit psychoactive activity and cardiovascular side effects and are potential clinical candidates in the treatment of diabetic cardiovascular and other complications.

MR and PM equally contributed to the manuscript.

M. Rajesh · P. Mukhopadhyay · S. Bátkai · M. Arif · Z. V. Varga · C. Mátyás · J. Paloczi · P. Pacher (✉)
Laboratory of Cardiovascular Physiology and Tissue Injury, National Institute On Alcohol Abuse and Alcoholism, National Institutes of Health, Bethesda, MD, USA
e-mail: pacher@nih.gov

Z. V. Varga
Department of Pharmacology and Pharmacotherapy, Semmelweis University, Budapest, Hungary

A. Lehocki
Departments of Hematology and Stem Cell Transplantation, South Pest Central Hospital, National Institute of Hematology and Infectious Diseases, Saint Ladislaus Campus, Budapest, Hungary

G. Haskó
Department of Anesthesiology, Columbia University, New York, NY, USA

Keywords Diabetes · Cardiomyopathy · Accelerated aging · Cannabinoid 2 receptor

Introduction

It has long been recognized that diabetes mellitus promotes accelerated aging [1–3]. Worldwide, the incidence of diabetes mellitus is increasing at an alarming rate, and it is predicted to accelerate further and reach epidemic proportions [4]. Cardiovascular complications are major contributors of the morbidity and mortality associated with uncontrolled glycemic levels in subjects with diabetes mellitus [4]. Since the initial description of cardiomyopathy by histopathological studies from the postmortem samples from subjects with diabetes mellitus, nearly three decades ago, there has been considerable progress made in defining diabetic cardiomyopathy (DCMP) as distinct clinical cardiovascular complication in the diabetic setting [5, 6]. Clinical epidemiological studies have revealed that development of DCMP could occur independent of comorbid risk factors such as hyperglycemia, hyperlipidemia, and/or hypertension[7], and diabetes-induced deterioration in the cardiac function is also one of the major causes for chronic heart failure. Although significant progress has been made in the development of therapeutic agents for the treatment of the above-mentioned underlying risk factors, the pathogenesis of DCMP is still largely elusive, and effective drugs to prevent and/or treat the cardiac injury in the diabetic milieu are not available. Therefore, it is important to delineate the pathological mechanisms of DCMP and to identify novel potential drug targets, which can be exploited for clinical utility in the management of DCMP.

Several mechanisms have been postulated for the development of DCMP; these include oxidative/nitrative stress, overactivation of renin–angiotensin system, aldose reductase, xanthine oxidase, and poly(ADP-ribose) polymerase (PARP) [7–10]. We have previously reported that cannabinoid receptor 1 (CB_1R) overactivation contributes to the development of DCMP in a murine model of diabetes [11].

Cannabinoid 2 receptor (CB_2R) activation in inflammatory cells and activated endothelium attenuates the pathological changes associated with atherosclerosis [12], myocardial infarction, stroke, and hepatic cardiomyopathy [13, 14]. In this study, we explored the role of CB_2R on the development of pathological changes associated of DCMP. Herein, we report that activation of CB_2R with selective agonist ameliorates the development of DCMP, via mitigating inflammation, oxidative/nitrative stress, cell death, and fibrosis.

Methods

Animals and treatment

Animal protocols used in this study adhered to the National Institutes of Health (NIH) guidelines and were approved by the Institutional Animal Care and use Committee of the National Institute on Alcohol Abuse and Alcoholism. Diabetes was induced in 8–12 weeks C57/BL6J(WT) (male, Jackson Laboratories, Bar Harbor, ME) or $CB_2^{-/-}$ (WT) and $CB2^{-/-}$ mice (generated at NIAAA/NIH) weighing 23–25 g via intra peritoneal (i.p.) administration of streptozotocin (STZ, Sigma chemicals, St Louis, MO) at the dose of 50 mg/kg dissolved in 100 mM citrate buffer pH 4.5 for 5 consecutive days. After 5 days, the blood glucose levels were measured using Ascensia Contour Glucometer (Bayer health care, NY) by mandibular puncture blood sampling. Mice which had blood sugar values > 250 mg/dl were used for the study [11, 15]. Control animals were administered with the same volume of citrate buffer, and all mice had access to food and water ad libitum. After diabetes was established, these mice were treated with selective CB_2 agonist JWH-133 [16] (10 mg/kg), i.p./day for 11 weeks (Fig. 1A, B). After 12 weeks, animals were sacrificed, and the hearts were excised and snap frozen in liquid nitrogen for biochemical determinations or fixed in formalin for histological evaluations.

Determination of cardiac function by pressure–volume conductance analysis

Left ventricular contractile performance was analyzed in anesthetized mice (with 2% isoflurane). Pressure–volume curves were analyzed, and maximal slope/rate of systolic pressure increment (+dP/dt), diastolic decrement (–dP/dt), ejection fraction (EF), cardiac output (CO), and stroke work (SW) were computed. For the indicator of diastolic function, the relaxation time constant (τ) was also calculated. Hemodynamic parameters were also determined under conditions of changing preload by transiently occluding the inferior vena cava (IVC) following

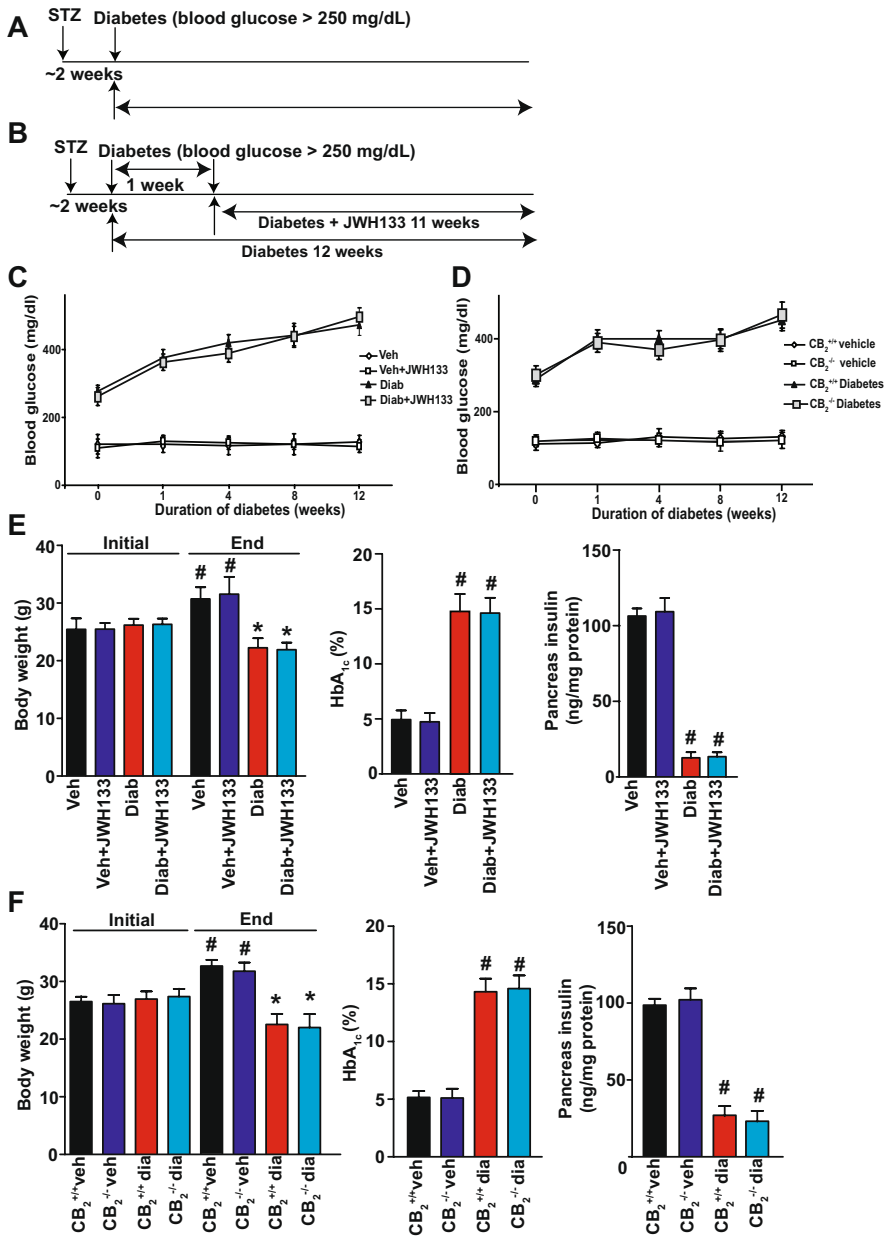

Fig. 1 Effect of diabetes on blood glucose, body weight, HbA1c levels, and pancreatic insulin content in $CB_2^{-/-}$ mice and JWH-133 treated WT diabetic mice. **A** Time scheme of diabetes induction. **B** Treatment scheme with the selective CB2 receptor agonist JWH133. **C** and **D** Blood glucose was monitored during the course of the study as described in the methods section. **E** and **F** Body weights were measured initially and after induction of diabetes periodically, and the data shown indicates the baseline and the final body weights in the respective groups. At the end of the study, EDTA whole blood was collected, and the glycosylated hemoglobin (HbA_{1C}) levels were determined as described in the Methods section. After the completion of the study, the pancreas was excised snap frozen in liquid nitrogen, and later, the insulin levels were determined using ELISA as described in the Methods section. #$P < 0.05$ vs. vehicle/JWH-133 (initial vs. end); *$P < 0.05$ vs. diabetes/diab + JWH-133 (initial vs. end), $n = 10–12$/group. #$P < 0.05$ vs. WT-vehicle/$CB2^{-/-}$ vehicle (initial vs. end); *$P < 0.05$ vs. WT diabetes/$CB2^{-/-}$ diabetes (initial vs. end), $n = 10–12$/group

thoracotomy. Additional preload-independent measures were evaluated including the dP/dt–end-diastolic volume (EDV) relation (dP/d–EDV) and the preload-recruitable stroke work (PRSW) [17].

Pancreatic insulin content

Pancreatic insulin content was determined using the kit obtained from ALPCO diagnostics (Salem, NH), by following the extraction procedure described previously [11, 15].

Determination of glycosylated hemoglobin (HbA_{1C})

Glycosylated hemoglobin (HbA_{1C}) levels in EDTA-treated whole blood samples were determined using the commercially available reagents procured from Stanbio laboratory (Boerne, TX) [11].

Reverse transcription and real-time PCR

Heart tissues were homogenized, and total RNA was isolated using Trizol LS reagent (Invitrogen, Carlsbad, CA) according to manufacturer's instruction. The RNA was treated with RNase-free DNase (Ambion, TX) to remove genomic DNA contamination. Total RNA was then reverse-transcribed to cDNA using the SuperScript II (Invitrogen), and the target genes were amplified using the standard real-time PCR kit (Applied Biosystems, Foster city CA). The amplification was performed in real-time PCR system (Applied Biosystems, CA) using the following conditions: initial denaturation at 95 °C for 2 min, followed by 35 cycles were performed at 95 °C for 30 s and 60 °C for 30 s. The fold induction/repression in gene expression by real-time RT-PCR was calculated after adjusting for actin using the formula $2^{-\Delta\Delta Ct}$. CB_2R expression was quantified using Qiagen primer in mouse brain, spleen, and heart as described previously [14, 18]. For other primer sequences, see prior publications [10, 11, 15].

Human RNA-seq data

Human RNA-seq data were obtained from the Genotype-Tissue Expression (GTEx) Project Portal on 02/08/2022 and dbGaP accession number phs000424.v8.p2 on 02/08/2022. TPM (transcript per-kilobase million) data were filtered to include the selected

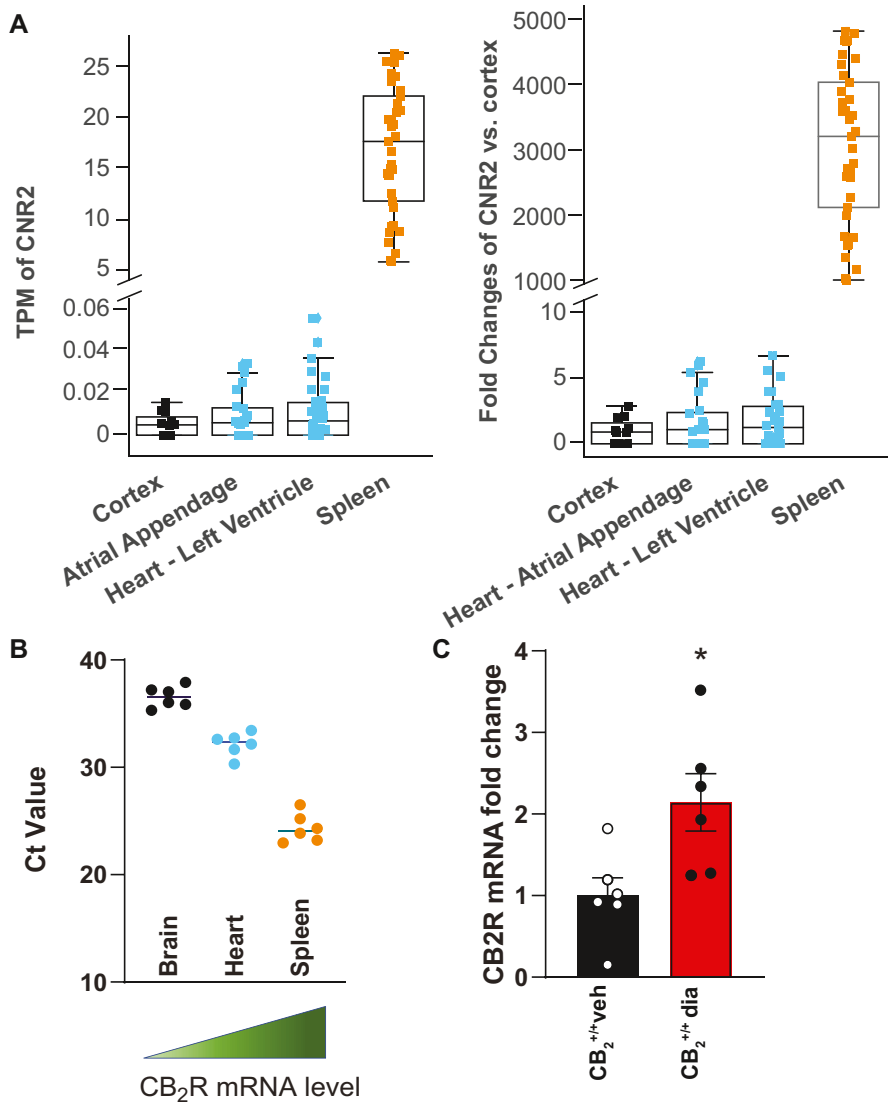

Fig. 2 Human or mouse cardiac CB_2R expression in normal or diabetic hearts. **A** Shows CNR2 gene expression in the human cortex ($n=11$: 7 male, 4 female), spleen ($n=37$: 25 male, 12 female), cardiac atrial appendages ($n=24$: 16 male, 8 female), and left ventricles ($n=34$: 22 male, 12 female) from healthy subjects. The results are shown both in TPM (transcript per-kilobase million) and fold changes compared to negative control cortex. The spleen was used as positive control for CNR2/CB2R expression. **B** Shows expression of CB_2R by RT-PCR in Ct values in mouse brain, heart, and spleen, $n=6$/group. **C** CB_2R expression in normal and diabetic mouse hearts, $n=6$

tissues from subjects with no history of heart diseases, i.e., myocardial infarction (variable ID: MHHRTATT), ischemic heart diseases (MHHRTDIS), other heart diseases (MHHRTDISB), and non-heart-related underlying cause of death (DTHFUCOD). Moreover, we excluded samples with procedure time > 22 h after time of death (TRISCH). The TPM values of each sample were normalized by the mean TPM of the cortex tissue to get the fold changes (Fig. 2). The significance levels were determined by using post hoc Tukey's test using the *statsmodel* package in Python 3.7.

Myocardial 4-hydroxynonenal (4-HNE) content

4-HNE in the myocardial tissues was determined using the kit (Cell Biolabs, San Diego). In brief, BSA or myocardial tissue protein extracts (10 µg/mL) were adsorbed on to a 96-well plate for 12 h at 4 °C. 4-HNE adducts present in the sample or standard are probed with anti-HNE antibody, followed by an HRP conjugated secondary antibody. The HNE–protein adduct content in an unknown sample is determined by comparing with a standard curve [11].

PARP activity

PARP activities in the myocardial tissue homogenates were performed using the universal colorimetric assay kit (Trevigen Inc., Gaithersburg, MD). In brief, the assay was based on determining the biotinylated poly(ADP-ribose) incorporation on to the histone proteins coated in ELISA wells [11].

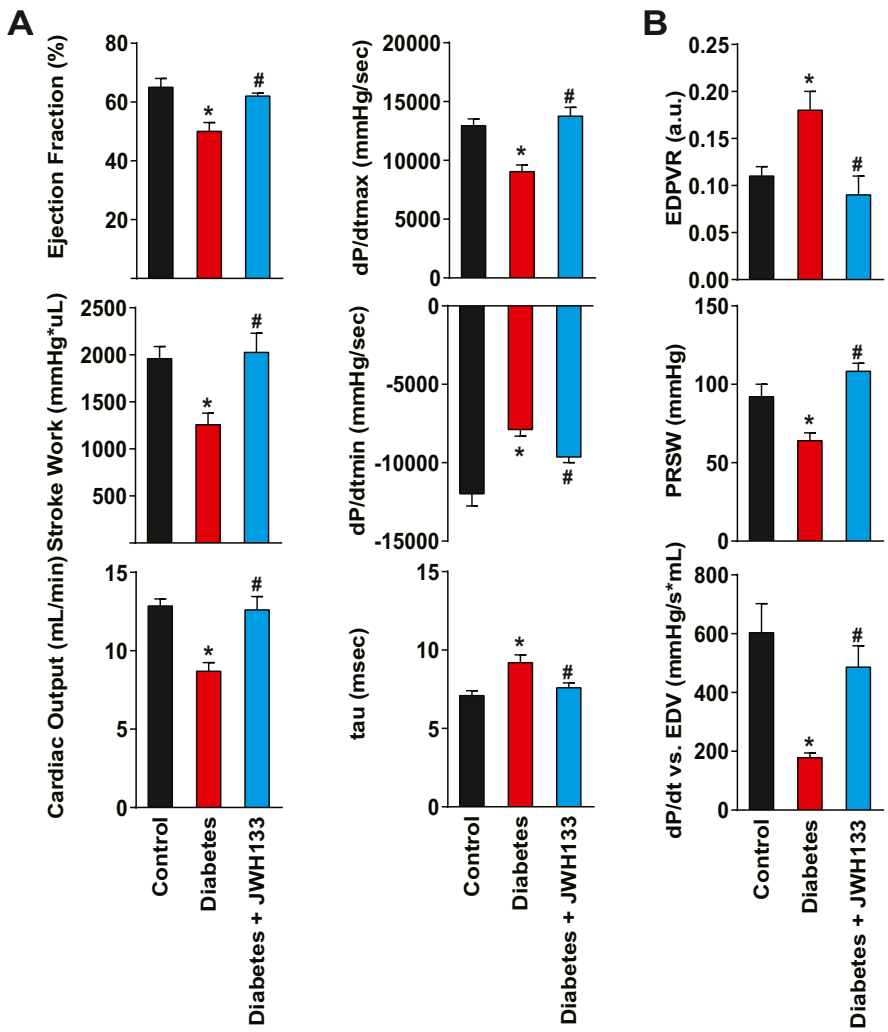

Fig. 3 Effect of diabetes and pharmacological CB_2R agonist JWH133 on myocardial contractile performance. **A** Shows steady-state contractile parameters in WT control, WT diabetic, and WT diabetic animals treated with the CB_2R agonist drug JWH133. **B** Depicts the effect of diabetes and JWH-133 treatment load-independent parameters of myocardial function. $^*P < 0.05$ vs. control; $\#P < 0.05$ vs. diabetes, $n = 6$. Data are presented as means ± SEM. dP/dtmax, maximal rate of ventricular pressure rise; dP/dtmin, maximal rate of ventricular pressure decline; tau (τ), isovolumetric relaxation time constant; dP/d–EDV, dP/dt–end-diastolic volume (EDV) relation; PRSW, preload-recruitable stroke work; and EDPVR, slope of end-diastolic PV relation

Caspase-3 activity

Caspase-3 activities in the myocardial tissue samples were performed using the Caspase-3 Assay Kit from BioVision (Mountain View, CA). In brief, the caspase-3 substrate p-nitroanilide (pNA)-bis-(N-CBZ-L-aspartyl-L-glutamyl-L-valyl-L-aspartic acid amide (DEVD-pNA) was added to the sample in the assay buffer provided and incubated in room temperature (RT) for 4 h. The caspase-3 in the samples cleaves the pNA from DEVD. The pNA light emission was quantified using microplate spectrophotometer (Molecular Devices, Sunnyvale, CA) [11].

DNA fragmentation

The quantitative determination of cytoplasmic histone-associated DNA fragments (mono- and oligonucleosomes) due to in vivo cell death was measured using the sandwich ELISA kit as per the protocol supplied by the vendor (Roche Diagnostics GmbH) [11, 15].

Myocardial 3-nitrotyrosine (3-NT) accumulation

Quantification of 3-NT levels in the heart tissues was performed using the sandwich ELISA kit as per the manufacturer-supplied protocol (Hycult Biotechnology, Uden, the Netherlands) [11, 15, 19].

Sirius red staining for collagen

Tissue sections were stained with picrosirius red stain solution for 1 h at RT. Then slides were washed in two changes of acidified water (0.5% acetic acid) for 2 min, and excess of water was removed by blotting. Finally, the sections were dehydrated in 100% alcohol and cleared in xylene and mounted with cover glass. Quantification of fibrosis was performed as reported by us previously [11].

Statistical analysis

All the values were represented as mean ± SEM. Statistical significance of the data was determined by ANOVA followed by Tukey's post hoc test for multiple comparison. The analysis was performed using the statistical software package (GraphPad Prism-V, CA). $P < 0.05$ was accepted as significant.

Results

Metabolic parameters

Induction of diabetes by multiple low doses of STZ leads to marked reduction in the body weights with concomitant increase in the blood glucose levels in the WT and $CB_2^{-/-}$ mice, respectively (Fig. 1F), while blood glucose levels were elevated and remained unchanged during 12 weeks study period in both wild-type and $CB_2^{-/-}$ mice

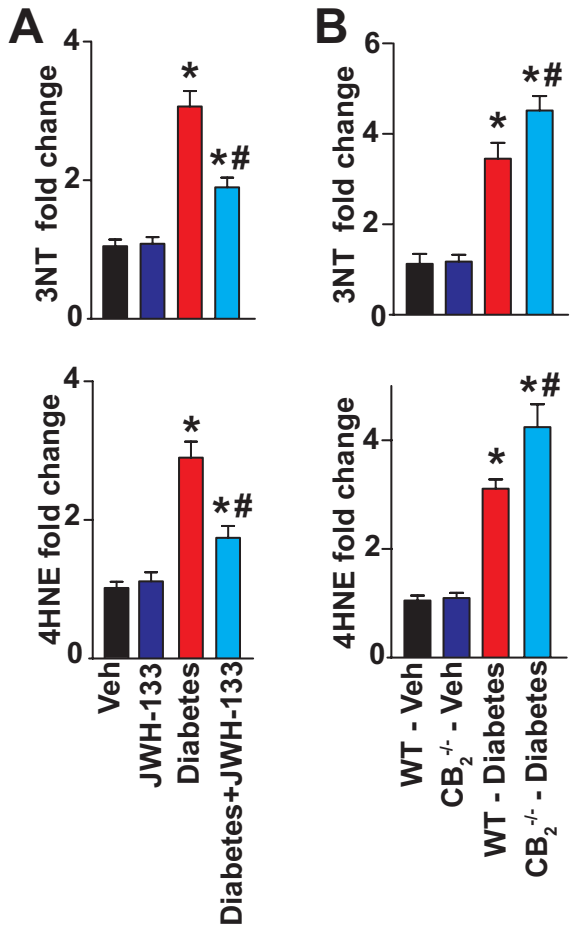

Fig. 4 Effect of diabetes and JWH-133 treatment on the myocardial oxidative/nitrative stress markers in WT and $CB2^{-/-}$ mice. **A** Depicts the effect of JWH-133 treatment on the oxidative/nitrative stress parameters, $*P < 0.05$ vs. Veh; $\#P < 0.05$ vs. diabetes, $n = 6$. **B** Genetic ablation of CB_2R results in exaggerated oxidative/nitrative stress in the diabetic myocardial tissues when compared with the WT diabetic animals $*P < 0.05$ vs. WT- vehicle treated animals; $\#P < 0.05$ vs. WT diabetic animals, $n = 6$. Data are presented as means ± SEM

(Fig. 1D). Determination of glycosylated hemoglobin (HbA_{1C}) an index for glycemic control at the end of the study showed marked elevation in the WT diabetic mice (Fig. 1E). Similar trend was observed in $CB_2^{-/-}$ mice (Fig. 1F). Induction of diabetes in WT and $CB_2^{-/-}$ mice exhibited diminished pancreatic insulin content (Fig. 1F). Treatment of WT mice with CB_2R agonist JWH-133 did not significantly affect blood glucose (Fig. 1C), HbA_{1C}, or pancreas insulin content (Fig. 1E).

Very low CNR2/CB_2R expression in normal human and mouse hearts and slight increase in diabetic myocardium

There was minimal expression of CNR2 gene in normal human heart atrial appendages and left ventricles, likewise in normal mouse hearts (Fig. 2A, B). There was slight increase in CB_2R expression in diabetic hearts, most likely originating from activated endothelium and infiltrating immune cells.

Diabetes-induced myocardial contractile dysfunction is attenuated in JWH-133-treated mice

Chronic diabetes (12 weeks after the induction by STZ) leads to diminished contractile performance in WT mice (Fig. 3). Among the steady-state load-dependent contractile parameters assessed, there was a significant reduction in left ventricular ejection fraction, myocardial stroke work, cardiac output, and dP/dtmax (maximal rate of left ventricular pressure rise). This impaired systolic function was also associated with decreased diastolic performance indicated by a decrease of dP/dtmin (maximal rate of ventricular pressure decline), prolongation of the isovolumic relaxation constant (tau), and increase of the slope of the end-diastolic pressure volume relationship (EDPVR) in diabetes (Fig. 3A, B). The load-independent parameters of myocardial contractile function, such as the preload-recruitable stroke work (PRSW) and linear slope of the dP/dtmax–EDV relationship, were also impaired (Fig. 3B). Treatment of WT diabetic mice with JWH-133 significantly attenuated the diabetes-induced systolic and diastolic dysfunction.

CB_2R agonist JWH-133 attenuates diabetes-induced myocardial oxidative and nitrative stress, which is exacerbated in $CB_2^{-/-}$ mice

Markers of oxidative/nitrative stress, such as 4-hydroxynonenal (4-HNE) (a stable product of lipid peroxydation) and 3-nitrotyrosine (3-NT) (a marker

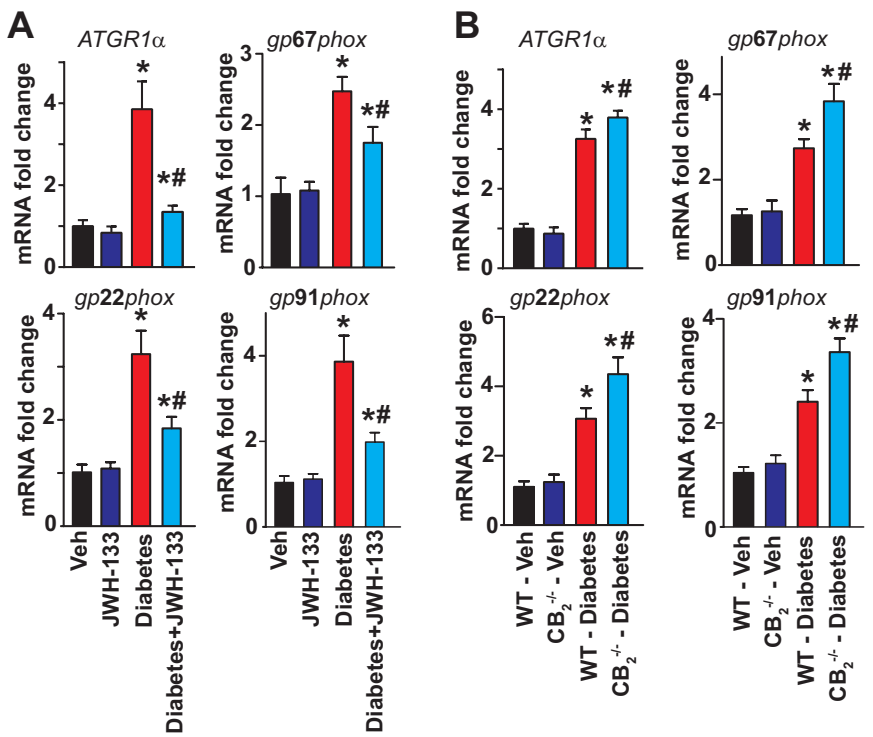

Fig. 5 Effect of diabetes and JWH-133 treatment on the myocardial mRNA expression of NADPH oxidase subunits and ATGR1α in WT and $CB2^{-/-}$ mice. **A** Depicts the mRNA expression of NADPH oxidase expression upon JWH-133 treatment in the myocardial tissues. $*P<0.05$ vs. Veh/JWH-133; $\#P<0.05$ vs. diabetes, $n=6$. **B** Shows the mRNA expression of NADPH oxidase subunits in the respective groups. $*P<0.05$ vs. WT-vehicle treated animals; $\#P<0.05$ vs. WT diabetic animals, $n=6$

of nitrative stress), were markedly elevated in WT diabetic myocardial tissues (Fig. 4), when compared with corresponding non-diabetic animals. Treatment of WT diabetic mice with JWH-133 attenuated the oxidative stress in these animals (Fig. 4A). There was a greater degree of elevation in the 3-NT and 4-HNE levels in the samples from $CB_2^{-/-}$ mice (Fig. 4B). Induction of diabetes leads to marked increases in the mRNA expression of NADPH oxidase subunits, such as gp22phox, gp67phox and gp91phox, and Agtr1α(angiotensin II receptor, type 1α) in WT diabetic hearts compared with WT non-diabetic animals (Fig. 5). All these pathological effects were attenuated by JWH-133 treatment of mice. There was enhanced NADPH oxidase and Agtr1αmRNA expression in diabetic $CB_2^{-/-}$ mice compared to WT diabetic animals (Fig. 5A, B).

CB_2R agonist JWH-133 attenuates diabetes-induced myocardial pro-inflammatory response and macrophage infiltration, which is exacerbated in $CB_2^{-/-}$ mice

Earlier studies have demonstrated the pivotal role of inflammation in the development of diabetic cardiomyopathy [11, 15]; therefore, the mRNA expression of inflammatory cytokines and chemokines such as TNF-α, IL1-β, MCP-1, MIP-1α, adhesion molecule ICAM-1, and F4/80 (marker of macrophage infiltration) was determined in the myocardial samples as indicated in respective groups (Fig. 6). TNF-α, IL1-β, MIP-1α, MCP-1, and F4/80 expressions were markedly elevated in WT diabetic myocardial tissues compared with WT non-diabetic mice (Fig. 6). Similarly, ICAM-1 expression was elevated in the hearts of WT diabetic mice compared with non-diabetic mice (Fig. 6).

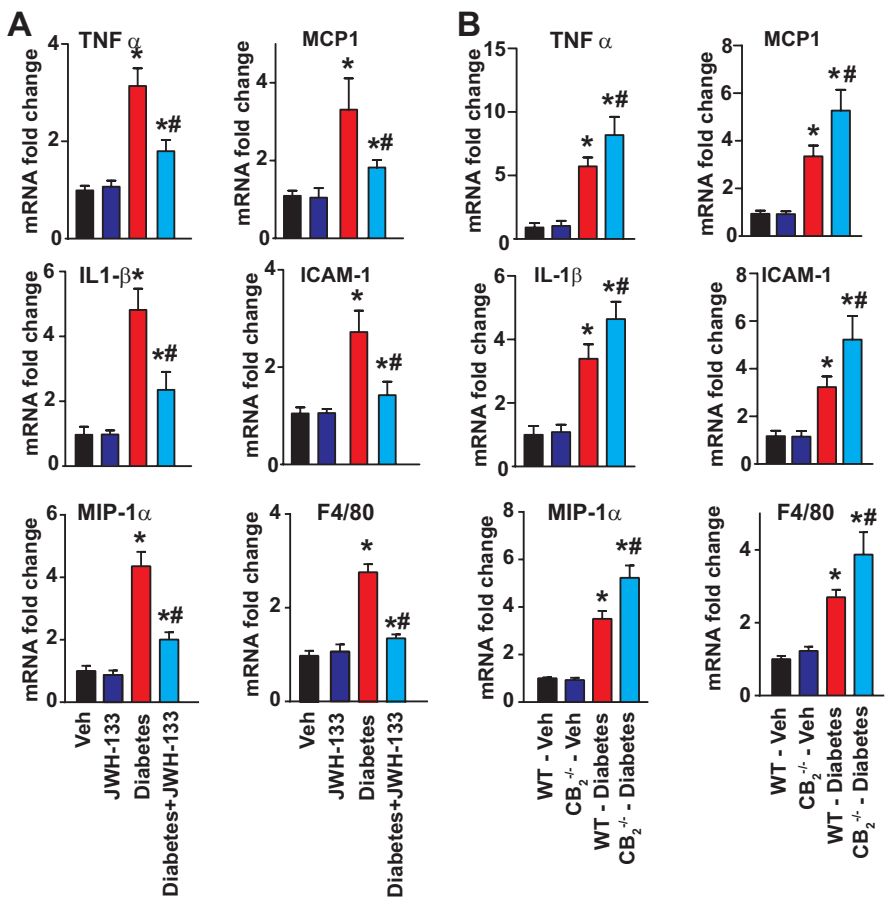

Fig. 6 Effect of diabetes and JWH-133 treatment on the myocardial inflammation in WT and $CB2^{-/-}$ mice. **A** Depicts the mRNA expression of pro-inflammatory cytokines/chemokines, adhesion molecules, and marker of macrophage infiltration upon JWH-133 treatment in the myocardial tissues. $^*P < 0.05$ vs. Veh/JWH-133; $\#P < 0.05$ vs. diabetes, $n = 6$. **B** Shows the mRNA expression of respective inflammatory markers in the myocardial tissues from the animal groups. $^*P < 0.05$ vs. WT-vehicle treated animals; $\#P < 0.05$ vs. WT diabetic animals, $n = 6$

Treatment of WT diabetic mice with a selective CB_2R agonist JWH-133 for 11 weeks mitigated the inflammation by diminishing the expression of pro-inflammatory markers (Fig. 6A). The changes in inflammatory cytokines and ICAM-1 were exacerbated in diabetic $CB_2^{-/-}$ mice compared with WT diabetic mice (Fig. 6B).

CB_2R agonist JWH-133 attenuates diabetes-induced myocardial remodeling and fibrosis, which is exacerbated in $CB_2^{-/-}$ mice

Diabetes-induced increased expression of pathological markers of myocardial remodeling (brain and atrial natriuretic peptides (BNP and ANP), myosin heavy chain (MHC) switch), which was attenuated by JWH133 and enhanced in $CB_2^{-/-}$ mice (Fig. 7A, B.)

Diabetes-induced myocardial fibrosis was first evaluated in the myocardial paraffin sections by Sirius red staining. There was significant collagen accumulation in the myocardial tissues from WT diabetic mice compared with WT non-diabetic animals (Figs. 8–9). Treatment of WT diabetic mice with JWH-133 mitigated myocardial fibrosis as indicated by diminished collagen accumulation (Fig. 8A) and the markers of fibrosis (Fig. 8B). There was enhanced myocardial fibrosis in $CB_2^{-/-}$ diabetic mice compared with WT diabetic mice (Fig. 9). Similar results were observed by evaluation of mRNA expression of multiple fibrosis markers in the myocardial tissues (Figs. 8–9B).

Enhanced diabetes-induced myocardial cell death in $CB_2^{-/-}$ mice and CB_2R agonist JWH-133 attenuates myocardial cell demise

The determination of cell death markers such as caspase-3/caspase-7, PARP activities, and chromatin fragmentation revealed significant elevations in the hearts of WT diabetic animals compared with their non-diabetic controls (Fig. 10). JWH-133 treatment of WT diabetic animals diminished myocardial apoptosis (Fig. 10A). The degree of cell death was more pronounced in $CB_2^{-/-}$ diabetic mice, compared with WT diabetic animals (Fig. 10B).

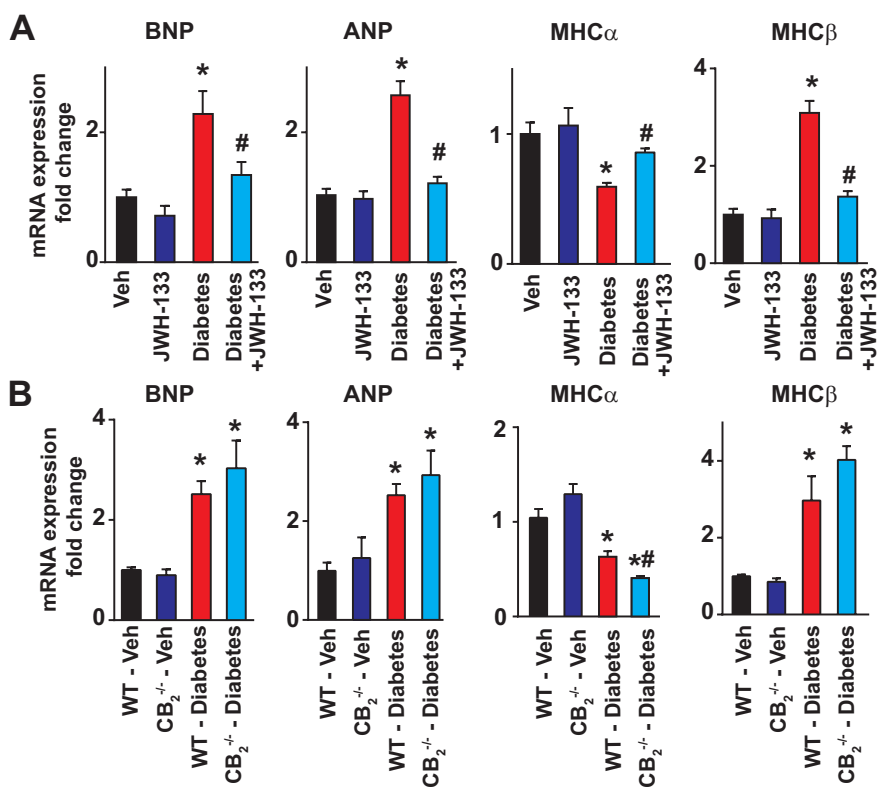

Fig. 7 Effect of diabetes and JWH-133 treatment on the myocardial markers of remodeling in WT and $CB2^{-/-}$ mice. **A** Shows the mRNA expression of myocardial remodeling markers and the effect of JWH133 treatments on these. $*P<0.05$ vs. Veh/JWH-133; $\#P<0.05$ vs. diabetes, $n=6$. **B** Depicts the mRNA expression of myocardial remodeling markers in the respective myocardial tissue samples. $*P<0.05$ vs. WT-vehicle treated animals; $\#P<0.05$ vs. WT diabetic animals, $n=6$

Discussion

Herein, we report that activation of CB_2R blunts diabetes-induced cardiac dysfunctions via amelioration of inflammation, oxidative stress, cell death, and fibrosis. Endocannabinoids are a group of bioactive lipids derived from arachidonic acid [20]. Principle endocannabinoids are anandamide and 2-arachidonoylglycerol [2-AG], and they act as physiological ligands for their cognate cannabinoid receptors — CB_1R and CB_2R, respectively [20]. CB_1R and CB_2R have been reported to be expressed in the rodent and human myocardium [12, 21]. However, often, these expression levels were based on the use of non-specific antibodies and/or unvalidated primers. In line with our findings, recent evidence suggests that in normal human and mouse heart, the expression of CB_2R is very low, and under pathological conditions, it predominantly originates from activated endothelium and infiltrating immune cells such as macrophages [13, 14, 22, 23]. CB_2R agonist does not exert direct cardiac or vascular effects under normal conditions but, under pro-inflammatory conditions, attenuates endothelial activation, chemotaxis, adhesion to the activated endothelium, and transmigration/activation of immune cells. The attenuation of vascular and general inflammation may contribute to improved endothelial function/microcirculation and to protective effects observed in animal models of atherosclerosis, myocardial infarction, stroke, sepsis,

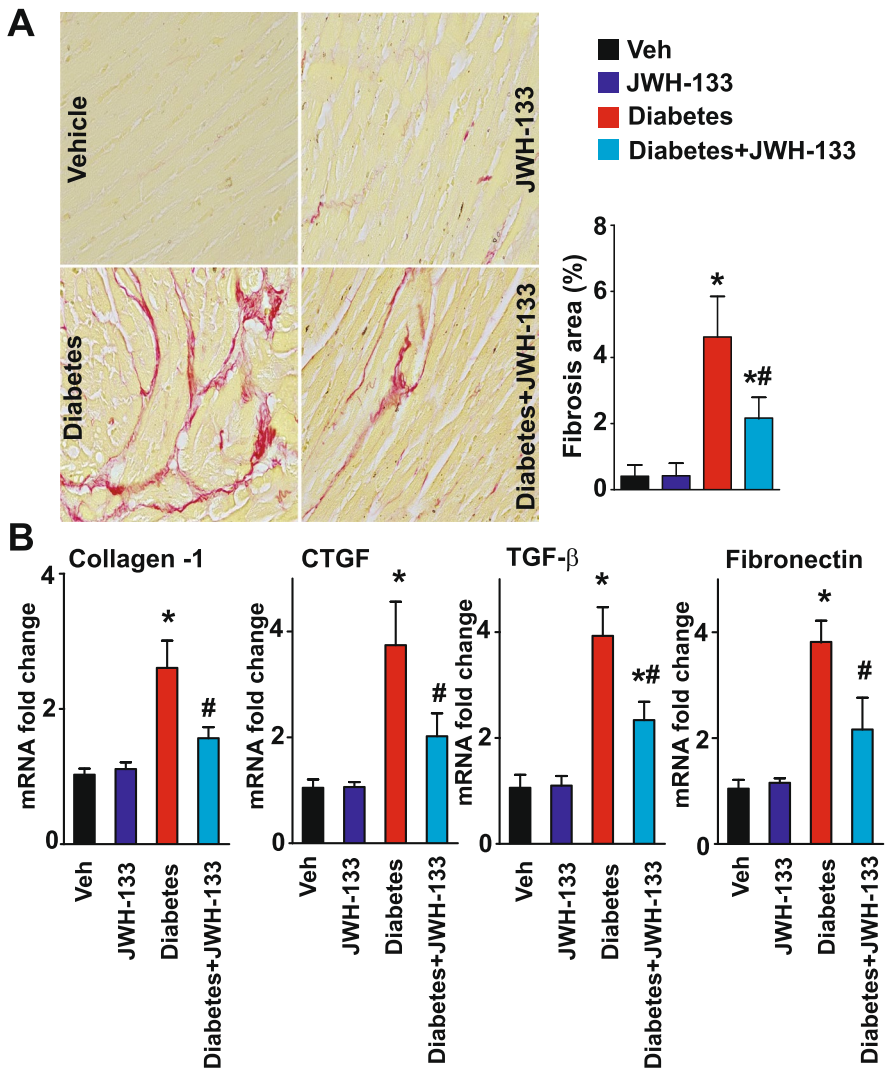

Fig. 8 Effect of JWH-133 treatment on diabetes-induced myocardial fibrosis in mice. **A** Representative images show Sirius red staining of the myocardial paraffin sections. The adjacent panel shows the quantification of fibrosis. $*P<0.05$ vs. Veh/JWH-133; $\#P<0.05$ vs. diabetes, $n=6$. **B** Depicts the mRNA expression of fibrosis markers in the myocardial tissue samples. $*P<0.05$ vs. Veh/JWH-133; $\#P<0.05$ vs. diabetes, $n=6$

and various cardiomyopathies [12, 13, 24]. In contrast to CB_2R, activation of CB_1R by endocannabinoids or synthetic ligands may directly or indirectly (through effects on sympathetic and parasympathetic nerves and central nervous system) modulate cardiovascular function [13, 25, 26]. Synthetic CB_1R agonists both in animals and humans may induce marked decrease of blood pressure and myocardial contractility [13, 20, 27]. In normal human and mouse hearts, there is a very low level of CB_1R expression in cardiomyocytes, endothelial cells, vascular smooth muscle, and fibroblast, which may be upregulated in pathological conditions (extreme obesity, various cardiomyopathies, and heart failure) [11, 28, 29]. In human endothelial cells and cardiomyocytes, CB_1R activation induces reactive oxygen species-dependent and species-independent activation of p38 and other mitogen activated protein kinases, facilitating cell death both in vitro and in vivo [30–33]. CB_1R activation in macrophages may also induce pro-inflammatory response, promoting atherosclerosis and other cardiovascular pathologies [34–36].

CB_1R activation has also been implicated in the development of diabetic cardiovascular complications, nephropathy, and retinopathy [11, 27, 30, 31, 37–39]. In the present study, utilizing a well-established model of diabetic cardiomyopathy [11, 15], we aimed to investigate the role of CB_2R in diabetic myocardium by using CB_2R agonist JWH133 and CB_2R knockout mice.

Previous studies have established that inflammation plays a key role in inducing cardiac dysfunction in the diabetic milieu. Hyperglycemia-induced activation of NFκB and subsequent production of pro-inflammatory cytokines (TNF-α, IL1-β)/chemokines (MCP-1) and adhesion molecules (ICAM-1 and VCAM-1) eventually culminates into the overproduction of reactive oxygen and nitrogen species (ROS/

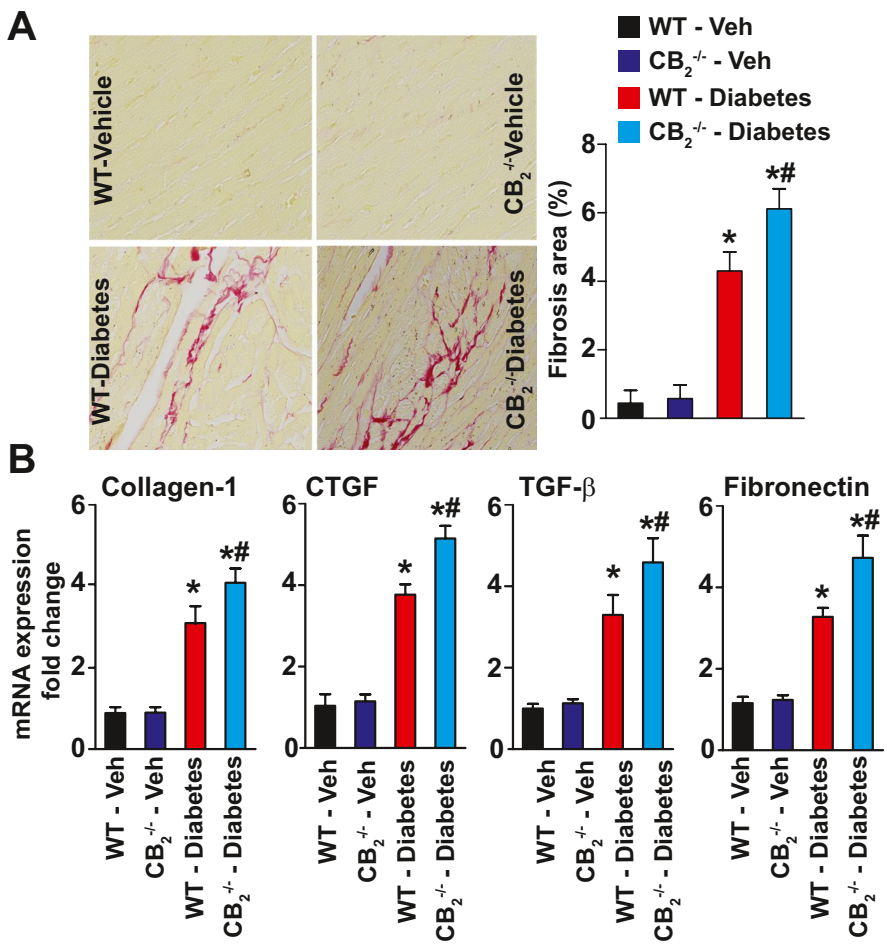

Fig. 9 Effect of diabetes-induced fibrosis in the myocardial tissues of $CB_2R^{-/-}$ mice. **A** Representative images show Sirius red staining of the myocardial paraffin sections. The adjacent panel shows the quantification of fibrosis. $^*P<0.05$ vs. WT-vehicle treated animals; $\#P<0.05$ vs. diabetes, $n=6$. **B** Depicts the mRNA expression of fibrosis markers in the myocardial tissue samples. $^*P<0.05$ vs. WT-vehicle treated animals; $\#P<0.05$ vs. WT diabetic animals, $n=6$

RNS) that profoundly affects cardiomyocyte contractility [11, 40]. The inhibition of inflammation has been documented to improve cardiac dysfunction in the diabetic heart [41]. In agreement with these findings, our results revealed increased expression of pro-inflammatory cytokines, chemokines, and adhesion molecules in the diabetic myocardial tissues and infiltrating macrophages, and this was markedly mitigated upon treatment with CB_2R selective agonist JWH133.

Oxidative/nitrative stress has been well-established in the development of diabetic cardiovascular complications [6–8]. Cumulative evidence indicates that mitochondria and NADPH oxidase are primary sources of the ROS generating apparatus in diabetic heart[7]. In our present study, we have also observed significantly enhanced expression of various NADPH oxidase isoforms in diabetic myocardial tissues, which paralleled with enhanced lipid-peroxidation and nitrative stress (4-HNE and 3-NT), respectively. Increased oxidative/nitrative stress was significantly attenuated by JWH133 treatment of diabetic mice. Hyperglycemia-induced myocardial cell demise has been recognized as major contributing factors in the loss of cardiac structure and function which eventually leads to heart failure [42]. Consistently with enhanced cardiomyocyte cell death in diabetes, we found increased caspase and PARP activities and chromatin fragmentation in diabetic hearts, which was attenuated upon treatment with JWH133.

Enhanced inflammation and oxidative stress trigger and perpetuate the development and progression of myocardial remodeling in the hyperglycemic environment via recruiting various pro-fibrotic mediators such as TGF-β, CTGF, fibronectin, and collagen-1, which result in extensive pathological extracellular matrix remodeling (overt fibrosis). This eventually further compromises myocardial contractile dynamics and results in heart failure [43]. Herein, we show the attenuation of myocardial fibrosis in the diabetic heart upon CB_2R activation with JWH133. Several previous studies have documented that activation of CB_2R resulted in the dampening of inflammation, oxidative/nitrative stress, apoptosis, and fibrosis in various pre-clinical models of cardiovascular diseases such as myocardial ischemia/reperfusion, atherosclerosis and restenosis [44–49], and hepatic cardiomyopathy [14], among others. Infiltration of inflammatory cells in the myocardium under hyperglycemic condition plays a key role in the initiation and propagation of oxidative stress, which promotes tissue damage [50, 51]. Several studies have previously reported that selective activation of CB_2R resulted in the repression of ROS generation via inhibition of NADPH oxidase and NFκB activation and inflammatory cytokine and adhesion molecule expression and blunted pro-apoptotic MAPKs in pre-clinical models of acute and chronic inflammation [12, 15, 22, 24]

In the present study, we have observed that diabetic $CB_2R^{-/-}$ mice exhibited aggravated oxidative stress, inflammation, apoptosis, and fibrosis when

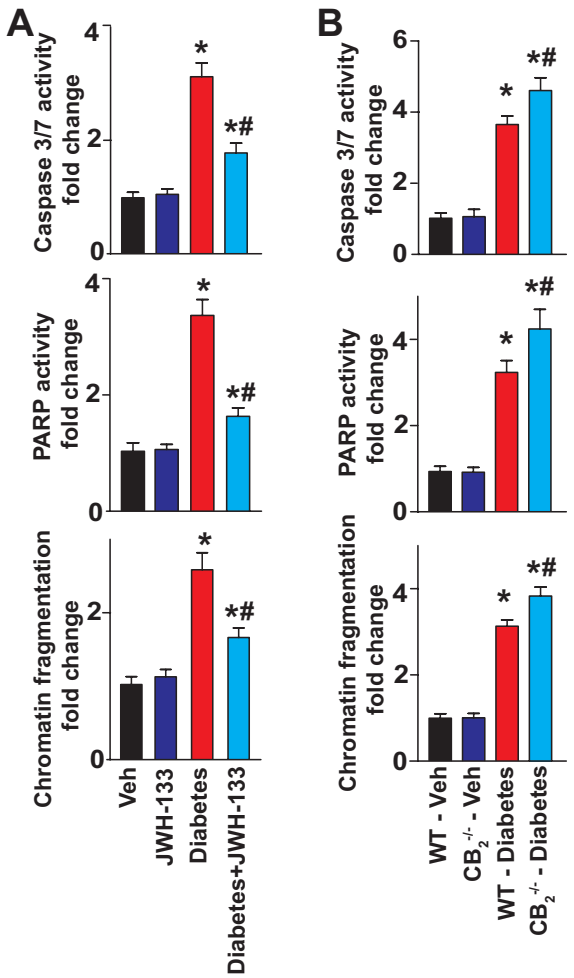

Fig. 10 Effect of diabetes and JWH-133 treatment on the myocardial markers of cell death in WT and $CB2^{-/-}$ mice. **A** Denotes the effect of JWH-133 treatment on the cell death markers in the myocardial tissues. $*P<0.05$ vs. Veh/JWH-133; $\#P<0.05$ vs. diabetes, $n=6$. **B** Shown are cell death markers in the respective groups. $*P<0.05$ vs. WT-vehicle treated animals; $\#P<0.05$ vs. WT diabetic animals, $n=6$

compared with WT diabetic mice, suggesting an important protective role of CB_2R in preventing diabetes-induced cardiac tissue injury. These results are also consistent with protective effect of CB_2R activation in diabetic nephropathy and aggravated kidney injury and fibrosis in diabetic $CB_2R^{-/-}$ mice [52, 53]. Interestingly, recent human clinical studies revealed that CB_2R expression and 2-AG levels were increased in myocardial tissues obtained from heart failure, suggesting the vital counter-regulatory role of CB_2R in mending the injured heart during chronic myocardial stress conditions [54].

In summary, we report that selective activation of CB_2R ameliorates diabetes-induced myocardial inflammation, tissue injury, and fibrosis and preserves the functional contractile capacity of the heart in the diabetic milieu. This is particularly encouraging, since unlike CB_1R agonists, CB_2R agonists do not elicit psychoactive and cardiodepressive side effects [13, 24]. Thus, targeting CB_2R with selective pharmacological agonists may emerge as a promising novel modality in the treatment of diabetic cardiomyopathy and other cardiovascular complications of diabetes.

Acknowledgements This study was supported by Intramural Research Program of NIH/NIAAA (to PP). ZVV is supported by the Rosztoczy Foundation. The Genotype-Tissue Expression (GTEx) Project was supported by the Common Fund of the Office of the Director of the National Institutes of Health and by NCI, NHGRI, NHLBI, NIDA, NIMH, and NINDS.

Author contribution MR, PM, GH, and PP designed the experiment. MR, PM, SB, CM, and AM performed the experiments. MR, ZVV, PM, AM, and CM performed the analysis. MR, ZVV, GH, AL, JP, and PP wrote/edited the paper.

Declarations

Competing interests The authors declare no competing interests.

References

1. Ryder JR, Northrop E, Rudser KD, Kelly AS, Gao Z, Khoury PR, Kimball TR, Dolan LM, Urbina EM. Accelerated early vascular aging among adolescents with obesity and/or type 2 diabetes mellitus. J Am Heart Assoc. 2020;9:e014891.
2. Cigolle CT, Blaum CS, Halter JB. Diabetes and cardiovascular disease prevention in older adults. Clin Geriatr Med. 2009;25:607–41, vii–viii.
3. Kirkman MS, Briscoe VJ, Clark N, Florez H, Haas LB, Halter JB, Huang ES, Korytkowski MT, Munshi MN, Odegard PS, Pratley RE, Swift CS. Diabetes in older adults. Diabetes Care. 2012;35:2650–64.
4. Milicevic Z, Raz I, Beattie SD, Campaigne BN, Sarwat S, Gromniak E, Kowalska I, Galic E, Tan M, Hanefeld M. Natural history of cardiovascular disease in patients with diabetes. Diabetes Care. 2008;31:S155–60.
5. Rubler S, Dlugash J, Yuceoglu YZ, Kumral T, Branwood AW, Grishman A. New type of cardiomyopathy associated with diabetic glomerulosclerosis. Am J Cardiol. 1972;30:595–602.
6. Liu Q, Wang S, Cai L. Diabetic cardiomyopathy and its mechanisms: role of oxidative stress and damage. J Diabetes Investig. 2015;5:623–34.
7. Varga ZV, Giricz Z, Liaudet L, Hasko G, Ferdinandy P, Pacher P. Interplay of oxidative nitrosative nitrative stress inflammation cell death and autophagy in diabetic cardiomyopathy. Biochim Biophys Acta (BBA) - Mole Basis Dis. 2015;1852:232–42.
8. Pacher P, Obrosova IG, Mabley JG, Szabo C. Role of nitrosative stress and peroxynitrite in the pathogenesis of diabetic complications Emerging new therapeutical strategies. Curr Med Chem. 2005;12:267–75.
9. Obrosova IG, Pacher P, SzabÃ C, Zsengeller Z, Hirooka H, Stevens MJ, Yorek MA. Aldose reductase inhibition counteracts oxidative-nitrosative stress and poly(ADP-ribose) polymerase activation in tissue sites for diabetes complications. Diabetes. 2005;54:234–42.
10. Rajesh M, Mukhopadhyay P, Bátkai S, Mukhopadhyay B, Patel V, Haskó G, Szabó C, Mabley JG, Liaudet L, Pacher P. Xanthine oxidase inhibitor allopurinol attenuates the development of diabetic cardiomyopathy. J Cell Mol Med. 2009;13:2330–41.
11. Rajesh M, Bátkai S, Kechrid M, Mukhopadhyay P, Lee W-S, Horváth B, Holovac E, Cinar R, Liaudet L, Mackie K, Haskó G, Pacher P. Cannabinoid 1 receptor promotes cardiac dysfunction, oxidative stress, inflammation, and fibrosis in diabetic cardiomyopathy. Diabetes. 2012;61:716–27.
12. Steffens S, Pacher P. Targeting cannabinoid receptor CB2 in cardiovascular disorders: promises and controversies. Br J Pharmacol. 2012;167:313–23.
13. Pacher P, Steffens S, Hasko G, Schindler TH, Kunos G. Cardiovascular effects of marijuana and synthetic cannabinoids: the good, the bad, and the ugly. Nat Rev Cardiol. 2018;15:151–66.
14. Matyas C, Erdelyi K, Trojnar E, Zhao S, Varga ZV, Paloczi J, Mukhopadhyay P, Nemeth BT, Hasko G, Cinar R, Rodrigues RM, Ait Ahmed Y, Gao B, Pacher P. Interplay of liver-heart inflammatory axis and cannabinoid 2 receptor signaling in an experimental model of hepatic cardiomyopathy. Hepatology. 2020;71:1391–407.
15. Rajesh M, Mukhopadhyay P, Bátkai S, Patel V, Saito K, Matsumoto S, Kashiwaya Y, Horváth B, Mukhopadhyay B, Becker L, Haskó G, Liaudet L, Wink DA, Veves A, Mechoulam R, Pacher P. Cannabidiol attenuates cardiac dysfunction, oxidative stress, fibrosis, and inflammatory and cell death signaling pathways in diabetic cardiomyopathy. J Am Coll Cardiol. 2010;56:2115–25.

16. Soethoudt M, Grether U, Fingerle J, Grim TW, Fezza F, de Petrocellis L, Ullmer C, Rothenhausler B, Perret C, van Gils N, Finlay D, MacDonald C, Chicca A, Gens MD, Stuart J, de Vries H, Mastrangelo N, Xia L, Alachouzos G, Baggelaar MP, Martella A, Mock ED, Deng H, Heitman LH, Connor M, Di Marzo V, Gertsch J, Lichtman AH, Maccarrone M, Pacher P, Glass M, van der Stelt M. Cannabinoid CB2 receptor ligand profiling reveals biased signalling and off-target activity. Nat Commun. 2017;8:13958.
17. Pacher P, Nagayama T, Mukhopadhyay P, Batkai S, Kass DA. Measurement of cardiac function using pressure-volume conductance catheter technique in mice and rats. Nat Protoc. 2008;3:1422–34.
18. Trojnar E, Erdelyi K, Matyas C, Zhao S, Paloczi J, Mukhopadhyay P, Varga ZV, Hasko G, Pacher P. Cannabinoid-2 receptor activation ameliorates hepatorenal syndrome. Free Radic Biol Med. 2020;152:540–50.
19. Varga ZV, Kupai K, Szucs G, Gaspar R, Paloczi J, Farago N, Zvara A, Puskas LG, Razga Z, Tiszlavicz L, Bencsik P, Gorbe A, Csonka C, Ferdinandy P, Csont T. MicroRNA-25-dependent up-regulation of NADPH oxidase 4 (NOX4) mediates hypercholesterolemia-induced oxidative/nitrative stress and subsequent dysfunction in the heart. J Mol Cell Cardiol. 2013;62:111–21.
20. Pacher P, Batkai S, Kunos G. The endocannabinoid system as an emerging target of pharmacotherapy. Pharmacol Rev. 2006;58:389–462.
21. Weis F, Beiras-Fernandez A, Sodian R, Kaczmarek I, Reichart B, Beiras A, Schelling G, Kreth S. Substantially altered expression pattern of cannabinoid receptor 2 and activated endocannabinoid system in patients with severe heart failure. J Mol Cell Cardiol. 2010;48:1187–93.
22. Rajesh M, Mukhopadhyay P, Batkai S, Hasko G, Liaudet L, Huffman JW, Csiszar A, Ungvari Z, Mackie K, Chatterjee S, Pacher P. CB2-receptor stimulation attenuates TNF-{alpha}-induced human endothelial cell activation, transendothelial migration of monocytes, and monocyte-endothelial adhesion. Am J Physiol Heart Circ Physiol. 2007;293:H2210-2218.
23. van Esbroeck ACM, Varga ZV, Di X, van Rooden EJ, Toth VE, Onodi Z, Kusmierczyk M, Leszek P, Ferdinandy P, Hankemeier T, van der Stelt M, Pacher P. Activity-based protein profiling of the human failing ischemic heart reveals alterations in hydrolase activities involving the endocannabinoid system. Pharmacol Res. 2020;151:104578.
24. Pacher P, Mechoulam R. Is lipid signaling through cannabinoid 2 receptors part of a protective system? Prog Lipid Res. 2011;50:193–211.
25. Pacher P, Batkai S, Kunos G. Cardiovascular pharmacology of cannabinoids. Handb Exp Pharmacol. 2005;599–625.
26. Batkai S, Pacher P. Endocannabinoids and cardiac contractile function: pathophysiological implications. Pharmacol Res. 2009;60:99–106.
27. Pacher P, Kunos G. Modulating the endocannabinoid system in human health and disease – successes and failures. FEBS J. 2013;280:1918–43.
28. Valenta I, Varga ZV, Valentine H, Cinar R, Horti A, Mathews WB, Dannals RF, Steele K, Kunos G, Wahl RL, Pomper MG, Wong DF, Pacher P, Schindler TH. Feasibility evaluation of myocardial cannabinoid type 1 receptor imaging in obesity: a Translational approach. JACC Cardiovasc Imaging. 2018;11:320–32.
29. Mukhopadhyay P, Batkai S, Rajesh M, Czifra N, Harvey-White J, Hasko G, Zsengeller Z, Gerard NP, Liaudet L, Kunos G, Pacher P. Pharmacological inhibition of CB1 cannabinoid receptor protects against doxorubicin-induced cardiotoxicity. J Am Coll Cardiol. 2007;50:528–36.
30. Mukhopadhyay P, Rajesh M, Batkai S, Patel V, Kashiwaya Y, Liaudet L, Evgenov OV, Mackie K, Hasko G, Pacher P. CB1 cannabinoid receptors promote oxidative stress and cell death in murine models of doxorubicin-induced cardiomyopathy and in human cardiomyocytes. Cardiovasc Res. 2010;85:773–84.
31. El-Remessy AB, Rajesh M, Mukhopadhyay P, Horvath B, Patel V, Al-Gayyar MM, Pillai BA, Pacher P. Cannabinoid 1 receptor activation contributes to vascular inflammation and cell death in a mouse model of diabetic retinopathy and a human retinal cell line. Diabetologia. 2011;54:1567–78.
32. Rajesh M, Mukhopadhyay P, Hasko G, Liaudet L, Mackie K, Pacher P. Cannabinoid-1 receptor activation induces reactive oxygen species-dependent and -independent mitogen-activated protein kinase activation and cell death in human coronary artery endothelial cells. Br J Pharmacol. 2010;160:688–700.
33. Tiyerili V, Zimmer S, Jung S, Wassmann K, Naehle CP, Lutjohann D, Zimmer A, Nickenig G, Wassmann S. CB1 receptor inhibition leads to decreased vascular AT1 receptor expression, inhibition of oxidative stress and improved endothelial function. Basic Res Cardiol. 2010;105:465–77.
34. Sugamura K, Sugiyama S, Nozaki T, Matsuzawa Y, Izumiya Y, Miyata K, Nakayama M, Kaikita K, Obata T, Takeya M, Ogawa H. Activated endocannabinoid system in coronary artery disease and antiinflammatory effects of cannabinoid 1 receptor blockade on macrophages. Circulation. 2009;119:28–36.
35. Immenschuh S. Endocannabinoid signalling as an anti-inflammatory therapeutic target in atherosclerosis: does it work? Cardiovasc Res. 2009;84:341–2.
36. Dol-Gleizes F, Paumelle R, Visentin V, Mares AM, Desitter P, Hennuyer N, Gilde A, Staels B, Schaeffer P, Bono F. Rimonabant, a selective cannabinoid CB1 receptor antagonist, inhibits atherosclerosis in LDL receptor-deficient mice. Arterioscler Thromb Vasc Biol. 2009;29:12–8.
37. Gruden G, Barutta F, Kunos G, Pacher P. Role of the endocannabinoid system in diabetes and diabetic complications. Br J Pharmacol. 2016;173:1116–27.
38. Jourdan T, Park JK, Varga ZV, Paloczi J, Coffey NJ, Rosenberg AZ, Godlewski G, Cinar R, Mackie K, Pacher P, Kunos G. Cannabinoid-1 receptor deletion in podocytes mitigates both glomerular and tubular dysfunction in a mouse model of diabetic nephropathy. Diabetes Obes Metab. 2018;20:698–708.
39. Barutta F, Corbelli A, Mastrocola R, Gambino R, Di Marzo V, Pinach S, Rastaldi MP, Perin PC, Gruden G. Cannabinoid receptor 1 blockade ameliorates albuminuria in experimental diabetic nephropathy. Diabetes. 2010;59:1046–54.

40. Westermann D, Van Linthout S, Dhayat S, Dhayat N, Schmidt A, Noutsias M, Song XY, Spillmann F, Riad A, Schultheiss HP and TschÃ¶pe C. Tumor necrosis factor-alpha antagonism protects from myocardial inflammation and fibrosis in experimental diabetic cardiomyopathy. Basic Research in Cardiology. 2007;102:500–7.
41. Westermann D, Walther T, Savvatis K, Escher F, Sobirey M, Riad A, Bader M, Schultheiss H-P and TschÃ¶pe C. Gene deletion of the kinin receptor B1 attenuates cardiac inflammation and fibrosis during the development of experimental diabetic cardiomyopathy. Diabetes. 2009;58:1373–81.
42. Johnson FL. Pathophysiology and etiology of heart failure. Cardiol Clin. 2014;32:9–19.
43. Mandavia CH, Aroor AR, DeMarco VG, Sowers JR. Molecular and metabolic mechanisms of cardiac dysfunction in diabetes. Life Sci. 2013;92:601–8.
44. Defer N, Wan J, Souktani R, Escoubet B, Perier M, Caramelle P, Manin S, Deveaux V, Bourin M-C, Zimmer A, Lotersztajn S, Fo Pecker, Pavoine C. The cannabinoid receptor type 2 promotes cardiac myocyte and fibroblast survival and protects against ischemia/reperfusion-induced cardiomyopathy. The FASEB Journal. 2009;23:2120–30.
45. Montecucco F, Matias I, Lenglet S, Petrosino S, Burger F, Pelli G, Braunersreuther V, Fo Mach, Steffens S, Di Marzo V. Regulation and possible role of endocannabinoids and related mediators in hypercholesterolemic mice with atherosclerosis. Atherosclerosis. 2009;205:433–41.
46. Montecucco F, Lenglet Sb, Braunersreuther V, Burger F, Pelli G, Bertolotto M, Mach FO, Steffens S. CB2 cannabinoid receptor activation is cardioprotective in a mouse model of ischemia/reperfusion. J Mole Cell Cardiol. 2009;46:612–20.
47. Hoyer FF, Steinmetz M, Zimmer S, Becker A, LÃ¼tjohann D, Buchalla R, Zimmer A and Nickenig G. Atheroprotection via cannabinoid receptor-2 is mediated by circulating and vascular cells in vivo. J Mole Cel Cardiol. 2011;51:1007–14.
48. Molica F, Matter CM, Burger F, Pelli G, Lenglet S, Zimmer A, Pacher P, Steffens S. Cannabinoid receptor CB2 protects against balloon-induced neointima formation. Am J Physiol Heart Circ Physiol. 2012;302:H1064–74.
49. Montecucco F, Di Marzo V, da Silva RF, Vuilleumier N, Capettini L, Lenglet SB, Pagano S, Piscitelli F, Quintao S, Bertolotto M, Pelli G, Galan K, Pilet L, Kuzmanovic K, Burger F, Pane B, Spinella G, Braunersreuther V, Gayet-Ageron AL, Pende A, Viviani GL, Palombo D, Dallegri F, Roux-Lombard P, Santos RAS, Stergiopulos N, Steffens S, Mach FO. The activation of the cannabinoid receptor type 2 reduces neutrophilic protease-mediated vulnerability in atherosclerotic plaques. Eur Heart J. 2012;33:846–56.
50. Pacher P, Szabo C. Role of peroxynitrite in the pathogenesis of cardiovascular complications of diabetes. Curr Opin Pharmacol. 2006;6:136–41.
51. Pacher P, Beckman JS, Liaudet L. Nitric oxide and peroxynitrite in health and disease. Physiol Rev. 2007;87:315–424.
52. Barutta F, Piscitelli F, Pinach S, Bruno G, Gambino R, Rastaldi MP, Salvidio G, Di Marzo V, CavalloPerin P, Gruden G. Protective role of cannabinoid receptor type 2 in a mouse model of diabetic nephropathy. Diabetes. 2011;60:2386–96.
53. Barutta F, Grimaldi S, Franco I, Bellini S, Gambino R, Pinach S, Corbelli A, Bruno G, Rastaldi MP, Aveta T, Hirsch E, Di Marzo V, Gruden G. Deficiency of cannabinoid receptor of type 2 worsens renal functional and structural abnormalities in streptozotocin-induced diabetic mice. Kidney Int. 2014;86:979–90.
54. Mohnle P, Schutz SV, Schmidt M, Hinske C, Hubner M, Heyn J, Beiras-Fernandez A, Kreth S. MicroRNA-665 is involved in the regulation of the expression of the cardioprotective cannabinoid receptor CB2 in patients with severe heart failure. Biochem Biophys Res Commun. 2014;451:516–21.